A Comparative Study of the Efficacy of Conventional Dissolved Gas Analysis Techniques, Fuzzy Inference Systems, and Artificial Neural Network Classifiers for Fault Diagnosis in Oil-Filled Power Transformers

Gomotsegang M Mokgosi, *SMSAIEE*, Cuthbert Nyamupangedengu, *MSAIEE*, and Ken J. Nixon, *FSAIEE, MIEEE*

***Abstract*— Power transformers are critical assets that require reliable monitoring due to their high economic and operational importance. Dissolved Gas Analysis (DGA) is extensively used as a condition monitoring technique because of its ability to detect internal faults without interrupting operation. However, its effectiveness is often constrained by reliance on expert knowledge and inconsistencies among traditional interpretation techniques. To address these challenges, this study explores the use of intelligent computational methods to enhance diagnostic accuracy. An Artificial Neural Network (ANN) model and Fuzzy Inference Systems (FIS) are evaluated using transformer DGA data. The ANN utilises a feedforward backpropagation algorithm with Bayesian regularization, while data preprocessing includes dimensionality reduction using Principal Component Analysis (PCA) and dataset balancing through Adaptive Synthetic Sampling (ADASYN). In parallel, fuzzy logic is incorporated into four conventional DGA approaches: IEC, Rogers, Doernenburg, and Duval Triangle to assess whether uncertainty handling improves classification performance. The proposed ANN model demonstrated improved classification performance reaching an accuracy of approximately 77% on unseen data, exceeding the performance of all conventional techniques. Among the fuzzy-enhanced methods, only the IEC approach demonstrated noticeable improvement. The findings indicate that ANN-based models offer a more reliable and consistent alternative for transformer fault diagnosis compared to both classical and fuzzy-modified techniques.**

***Index Terms*—Dissolved Gas Analysis, Power Transformer, Machine Learning, Artificial Neural Network, Fuzzy Inference Systems**

Open License: CC-BY

I. Introduction

Power transformers in operation experience combined mechanical forces, electrical disturbances, and thermal loading conditions that contribute to insulation degradation. Although they are designed to tolerate such conditions, prolonged exposure leads to insulation degradation and eventual failure. Faults inside transformers can range from minor partial discharges to severe arcing conditions, with each failure mode generating distinct gaseous by-products within the insulating oil. These degradation processes result in the release of characteristic gases such as hydrogen, methane, ethane, ethylene, and acetylene. Dissolved Gas Analysis (DGA) is commonly employed for transformer condition monitoring due to its affordability, reliability, and ability to diagnose faults without interrupting operation. Nevertheless, traditional DGA methods exhibit limitations, including ambiguity in fault classification [1][2], reduced effectiveness in complex fault scenarios [1], inconsistent outcomes across different diagnostic methods, as well as overlapping and undefined regions when distinguishing between high and low energy discharge faults [3]. Such limitations may result in delayed or inaccurate maintenance decisions. The contemporary approaches to improve DGA diagnosis have been the use of Artificial Intelligence (AI). Various AI models have been used by researchers in DGA based diagnosis of oil-filled power transformers. The approaches in the use of AI-based DGA diagnosis range from direct raw data input to AI models for fault recognition to various complex integrated architectures. Figure 1 illustrates possible architecture, and these are explored in this article.

G. Mokgosi was with the School of Electrical and Information Engineering, University of the Witwatersrand, Johannesburg, South Africa. She is now with Exxaro Resources (e-mail: gomotsegang.mokgosi@gmail.com).

C. Nyamupangedengu is with the School of Electrical and Information Engineering, University of the Witwatersrand, Johannesburg, South Africa (e-mail: cuthbert.nyamupangedengu@wits.ac.za).

K.J. Nixon is with the School of Electrical and Information Engineering, University of the Witwatersrand, Johannesburg, South Africa (e-mail: ken.nixon@wits.ac.za).

Various scholars have explored different types of AI models to improve the accuracy of DGA based transformer condition assessment. Common AI models used with various levels of success include Artificial Neural Network (ANN), Fuzzy Logic (FL), Neuro-Fuzzy Logic (NFL), Genetic, Hidden Markov Model (HMM), Support Vector Machine (SVM), Expert Systems, Hybrid Systems and Graphical Techniques [4]. Among these AI techniques, the ANN and FL techniques are particularly attractive as reviewed in the next section.

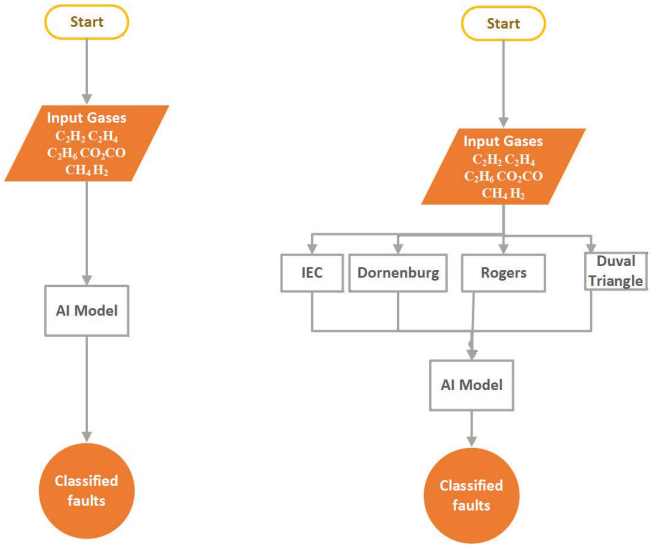

Fig. 1. Examples of integration architectures of AI models and DGA classical interpretation methods

This paper extends and significantly expands work previously presented at SAUPEC 2025 [5].

II. A REVIEW OF ANN AND FUZZY LOGIC MODELS INTEGRATION WITH DGA

The ANN machine learning tools are known for robustness, ability to handle nonlinear data sets, and resilience to inconsistencies in input data. Compared to other AI models in the context of DGA, as a non-parametric classifier, ANN has been found to outperform linear classifiers on new datasets. Ghoneim et al [4], used the Smart Fault Diagnostic Approach (SFDA) to improve DGA classification by integrating outputs from five conventional methods into a multilayer feed-forward ANN with backpropagation. This addressed some limitations of conventional DGA methods. The various cases of some degree of successes reported in the literature on the use of ANN in improving DGA inspired the present research with the focus being to explore an ANN model in comparison with the classical DGA methods using same original data set. Part of the findings were published in the proceedings of the 33rd Southern African Universities Power Engineering Conference (SAUPEC) [5] and in a Master's thesis [6]. The findings were that ANN had an average accuracy of 76.8% compared to lower accuracies in the conventional DGA techniques.

In other cases, reported in the literature [7, 8], ANFIS, a hybrid of ANN and Fuzzy Logic, combines the rule-based reasoning of Fuzzy Inference Systems (FIS) with ANN's learning capabilities, to effectively enhance accuracy and diagnosis of multiple faults. A rough set fuzzy wavelet ANN [9] was developed to reduce training time, simplify input data dimensions, and improve generalization, with ensemble learning methods suggested for better fault prediction.

FL is a well-established classification method with strong performance in transformer fault diagnosis. It handles uncertainty by allowing faults to belong to multiple categories simultaneously, reflecting varying degrees of severity. FL is particularly effective at managing overlapping data clusters and boundary uncertainties, distinguishing primary faults from secondary ones [10,11,12], and assessing fault severity [13]. It performs well in cases where ratio-based methods become ambiguous or undefined, such as near threshold limits or with multiple concurrent faults. Compared to ANN, FL uses a simpler, more interpretable linguistic decision-making approach, making it more transparent and practical for application [7]. One of the main limitations of fuzzy logic is that its setup often relies on a trial-and-error approach. Defining membership functions, selecting appropriate rules, and tuning parameters typically require repeated adjustments and expert judgment, which can be time-consuming and may reduce the consistency and reliability of the model.

Fuzzy Logic has been integrated with conventional DGA techniques such as Doernenburg, Key Gas [10,14], IEC, Rogers, and Duval [10] to enhance the diagnosis of incipient faults. A Fuzzy Inference Systems (FIS) approach of pre-conditioning data before input to an AI classifier has been successfully used before as reported in the literature [10,5,15]. The technique is useful in addressing the challenge of unclassified ranges in the ratio methods, which are often associated with multiple fault conditions. As an example, FIS was combined with the IEC ratio method (Fuzzy-IEC) in [10] to both detect incipient transformer faults to quantify their severity.

Among the alternative approaches to AI integration with DGA ratio methods, ANN and FL top the list. A question, however, arises about which of the two is better. Such an evaluation requires applying each of the two models to the same DGA data.

The rest of the article is structured as follows. Firstly, the nature of data preprocessing used in the study is presented followed by a review of the DGA gas ratio methods. The strengths and weaknesses of each technique are highlighted. The section on the application of the Fuzzy Logic model is presented and the results compared with those of the classical DGA ratio. Finally, the approach of integrating ANN on the same data set is presented and results compared with both the Fuzzy and DGA ratio methods. Conclusions are then presented.

III. DATA PREPARATION

The study utilised a dataset consisting of 145 transformer oil samples obtained from IEC TC 10 sources [16] and related publications. To address class imbalance and enrich the training

data, the ADASYN method was applied, increasing the dataset to 273 samples. The data was partitioned into training, validation, and testing subsets using a 70:20:10 allocation.
Each observation contains five input parameters corresponding to dissolved gas concentration levels and associated fault classification outputs. Based on IEC 60599 classification, the fault categories considered are normal ageing (N), low-temperature thermal faults (TL < 300 °C), high-temperature thermal faults (TH > 300 °C), partial discharge (PD), and arcing (D).
In Table I and the following subsections, each of the classical DGA classification methods is explained.

A. IEC Method

The IEC method is based on three gas ratio calculations listed below (1-3) to evaluate dissolved gases and identify six major fault types as presented in Table I [3].

$$IEC1 = \frac{C_2H_2}{C_2H_4} \quad (1)$$

$$IEC2 = \frac{CH_4}{H_2} \quad (2)$$

$$IEC3 = \frac{C_2H_4}{C_2H_6} \quad (3)$$

The IEC method like the other ratio techniques also experiences limitations when the diagnostic values fall outside the defined ranges. This issue is often caused by the presence of multiple faults or emergence of the new fault combined with elevated background gas levels [1].

TABLE I: DGA ratio methods and corresponding fault types [17]

Method	F1 Thermal Fault (Cellulose)	F2 Thermal Fault (Oil)	F3 Electrical Fault (Corona)	F4 Electrical Fault (Arcing)
Rogers Ratio	Thermal fault <150°C	Thermal fault 300 - 700°C	Low energy electrical discharge	High energy electrical discharge
	Thermal fault 150–300°C	Thermal fault >700°C		
IEC Ratio	Thermal fault <150°C	Thermal fault 300 - 700°C	Low energy electrical discharge	High energy electrical discharge
	Thermal fault 150–300°C	Thermal fault >700°C		
Dornemburg Ratio	Thermal decomposition	Thermal decomposition	Low energy electrical discharge	High energy electrical discharge
Duval Triangle	Thermal Fault <300°C	Thermal Fault >300°C	Partial Discharge Mix Thermal and Electrical Faults	High energy Discharge

B. The Doernenburg Method

The Doernenburg method uses four ratios as listed in (4-6) to identify six types of faults, as summarised in Table I:

$$D1 = \frac{CH_4}{H_2} \quad (4)$$

$$D2 = \frac{C_2H_2}{CH_4} \quad (5)$$

$$D3 = \frac{C_2H_6}{C_2H_2} \quad (6)$$

The Doernenburg ratio method is regarded as applicable when the concentrations of H_2, CH_2, C_2H_2, and C_2H_4 exceed twice their respective threshold values while C_2H_6 exceeds three times the specified limit [17].

E. Evaluating the Dataset using DGA Techniques

This section evaluates the dataset using Rogers, Duval, Doernenburg and IEC methods and compares the results to the actual verified condition of the transformers. A total of 27 randomly selected samples were evaluated on DGA methods,

C. Rogers Method

Roger's ratio uses four ratios to diagnose fault conditions including partial discharge, as well as electrical and thermal faults of varying severity levels.

$$R1 = \frac{C_2H_2}{C_2H_4} \quad (7)$$

$$R2 = \frac{CH_4}{H_2} \quad (8)$$

$$R3 = \frac{C_2H_6}{CH_4} \quad (9)$$

$$R4 = \frac{C_2H_4}{C_2H_6} \quad (10)$$

The Rogers method, similar to the Doernenburg and IEC ratio techniques, also encounters challenges with the out-of-range diagnostic values.

D. Duval Triangle

The Duval triangle detects six types of fault gases using a triangular graphical diagram. The faults are classified into electrical, thermal, or combined electrical thermal categories. Equations (11-13) show the three ratios used by Duval triangle 1 to classify faults.

$$\%CH_4 = \frac{CH_4}{(CH_4+C_2H_2+C_2H_4)} \quad (11)$$

$$\%C_2H_2 = \frac{C_2H_2}{(CH_4+C_2H_2+C_2H_4)} \quad (12)$$

$$\%C_2H_4 = \frac{C_2H_4}{(CH_4+C_2H_2+C_2H_4)} \quad (13)$$

Among conventional DGA techniques, the Duval triangle is widely regarded as the most accurate [13][18] however its use is not recommended for samples with low gas concentrations, as it tends to classify a fault condition even in the absence of an actual fault. The method was developed to address the issue of undefined diagnostic ranges associated with ratio methods [5], and it has been reported to achieve superior fault classification accuracy with a high rate of correct predictions [4]. Figure 2 shows a Duval Triangle 1 that was used in the present study.

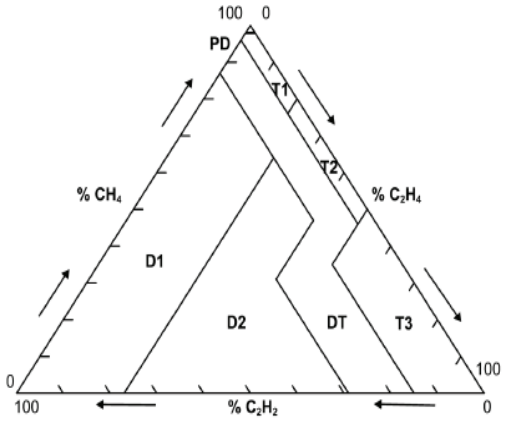

Fig. 2. Graphical representation of Duval Triangle 1

and the results compared against the actual condition as shown in Table II. Among the conventional techniques, the Doernenburg method achieved the best performance with Duval triangle being second best. It is widely reported in the literature that the Duval Triangle method consistently produces

a fault diagnosis, even for samples representing normal conditions with low gas concentrations. The IEC technique performed relatively poorly with most outputs falling out of range.

TABLE II: *Comparative accuracy of DGA methods on the dataset* (Reproduced with permission from IEEE, (Adapted from [5], © IEEE [2026])

Fault	No. Of Samples	IEC	Dorn	Duval	Rogers
PD	3	67%	100%	0%	67%
D	4	75%	75%	100%	50%
TL	6	17%	0%	0%	0%
TH	8	0%	100%	100%	75%
N	6	0%	0%	0%	0%
Average		32%	55%	40%	38%

The interpretation of various DGA ratio techniques are presented in Table I. Tables II and III show the accuracy results per fault type for the four DGA methods applied on the dataset. Doernenburg achieved an accuracy of 55% while IEC method recorded the lowest accuracy at 32% on the test dataset. The IEC performance is largely due to its limited defined classification regions, with a significant portion remaining undefined, which results in most predictions being classified as undefined.

IV. Evaluating Fuzzy Logic on the DGA Dataset

For the fuzzy logic approach used in the present work, the Mamdani based type 1 FIS was used on all simulations. The five input gases are initially converted into ratios according to each individual DGA method, namely IEC, Rogers, Doernenburg, and the Duval Triangle. These gas ratios are subsequently used as inputs to the fuzzy model.

The model employs triangular (IEC Method) and trapezoidal (Doernenburg, Rogers and Duval) membership functions, which are represented by (14) and (15), respectively.

$$f(x;a,b,c) = \begin{Bmatrix} 0, x \le a \\ \frac{x-a}{b-a}, a \le x \le b \\ \frac{c-x}{c-b}, b \le x \le c \\ 0, c \le x \end{Bmatrix} \tag{14}$$

Where x is the input variable/ratio being evaluated, a is the lower bound of the triangle, b is the peak point of the triangle and c is the upper bound of the triangle.

$$\mu(x;a,b,c,d) = \begin{cases} 0 & x \le a \\ \dfrac{x-a}{b-a} & a < x \le b \\ 1 & b < x \le c \\ \dfrac{d-x}{d-c} & c < x \le d \\ 0 & x \ge d \end{cases} \tag{15}$$

Where x is the input variable/ratio being evaluated, a, b, c and d being the edges of the rectangular membership function.

TABLE III: Comparative accuracy of DGA methods on actual transformer condition (Adapted from [5], © IEEE [2026])

Sample No	H2	CH4	C2H6	C2H4	C2H3	IEC Faultcode	Dorn Faultcode	Duval Faultcode	Rogers Faultcode	Actual Fault	Predicted Fault
Sample 1	227	759	156	3133	191	NA	TH	TH	TH	TH	TH
Sample 2	170	320	53	520	3	NA	TH	TH	TH	TH	TH
Sample 3	650	53	34	20	0	PD	PD	TH	PD	PD	PD
Sample 4	300	490	180	360	95	NA	TH	TH	NA	TH	D
Sample 5	117	167	48	481	7	NA	TH	TH	TH	TL	TH
Sample 6	307	22	2	33	109	NA	NA	D	NA	D	PD
Sample 7	60	144	67	449	9	NA	TH	TH	TH	TL	TL
Sample 8	208	1774	408	1431	1	NA	TH	TH	TH	TL	TL
Sample 9	75	15	7	14	26	D	D	D	NA	D	D
Sample 10	1230	163	27	233	692	D	D	D	D	D	D
Sample 11	755	229	32	404	460	D	D	D	D	D	D
Sample 12	105	125	71	166	10	NA	TH	TH	TH	N	PD
Sample 13	80	0	200	100	4	PD	NA	TH	PD	N	N
Sample 14	125	100	100	150	20	D	NA	TH	NA	N	TH
Sample 15	50	30	0	0	5	D	NA	D	NA	N	N
Sample 16	144	13	36	3	2	NA	PD	D	NA	PD	PD
Sample 17	503	40	25	14	0	PD	PD	TH	PD	PD	PD
Sample 18	246	596	322	872	3	NA	TH	TH	TH	TL	TL
Sample 19	1245	3865	721	2449	12	NA	TH	TH	TH	TL	TL
Sample 20	35	78	29	210	5	NA	TH	TH	TH	TL	N
Sample 21	546	1367	228	1196	14	NA	TH	TH	TH	TH	TL
Sample 22	334	872	221	1481	37	NA	TH	TH	TH	TH	TH
Sample 23	70	235	96	369	7	NA	TH	TH	TH	TH	TH
Sample 24	730	1588	431	3972	74	NA	TH	TH	TH	TH	TH
Sample 25	360	2933	23292	21341	94	TL	TH	TH	NA	TH	TH
Sample 26	52	31	3	1	5	TL	NA	D	NA	N	N
Sample 27	107	91	79	157	36	D	NA	TH	NA	N	N

Legend	
Colour	Meaning
Green	Correct Predictions
Red	Incorrect predictions
Grey	no output

The crisp input values are fuzzified into membership functions categorized as low, medium, high, and very high. Fault-specific rules are then generated according to the individual DGA techniques parameters. The COG (Centre of gravity) de-fuzzifier converts the membership functions back into crisp outputs using (16).

$$Z^* = \frac{\int z\mu(z)dz}{\int \mu(z)dz} \tag{16}$$

Where z represents the output variable over which the fuzzy set is defined, μ(z) is the membership function value at point z, and Z* is the de-fuzzified output representing the center of gravity of the fuzzy set.

A. *Fuzzy applied to the IEC ratio method*

In the IEC method, a triangular membership function as defined in (14) was used. The ratios from (1-3) were used as inputs to

the fuzzy logic model. These inputs were then fuzzified into linguistic categories such as Low, Medium, and High, allowing the model to interpret them effectively. For example, the following rules were configured:

R1: Low, R2: Low, R3: Low → Partial Discharge (PD)
R1: Low, R2: Medium, R3: High → Thermal Fault of Low Energy (TL)
R1: Low, R2: High, R3: High → Thermal Fault of High Energy (TH)

In total, 23 rules were established to define classification boundaries and identify fault types. Figure 3 illustrates the rule combinations and corresponding outputs. The output also employs a triangular membership function to classify conditions into five distinct fault categories.

In the example shown in Figure 3, the input values are R1 = 2, R2 = 0.5, and R3 = 4. The fuzzy model produces an output value of 3, which is then de-fuzzified using the Center of Gravity (COG) method. This corresponds to fault type 3, classified as a discharge fault.

B. Fuzzy applied to Duval Triangle method

For the Duval triangle method, a trapezoidal membership function, was applied. The three ratio inputs in (11-13) served as inputs to the fuzzy logic model. These inputs were then fuzzified into linguistic terms Low, Medium, and High corresponding to the ratios to enable interpretation by the model. Below is an example of the configured rules:

%CH_4 low, %C_2H_4 low, and %C_2H_2 low = Thermal Fault of low Energy (TL)
%CH_4 High, %C_2H_4 *N/A, and %C_2H_2 *N/A = Partial Discharge (PD)
%CH_4 *N/A, %C_2H_4 Med, and %C_2H_2 Vey High = Discharge (D)
*Note: N/A symbolizes that, regardless of the output condition.

A total combination of 26 rules was configured to define classification boundaries and determine fault types. Figure 4 shows the combination of rules used with the output. The output also uses triangular membership function to classify to 5 different conditions.

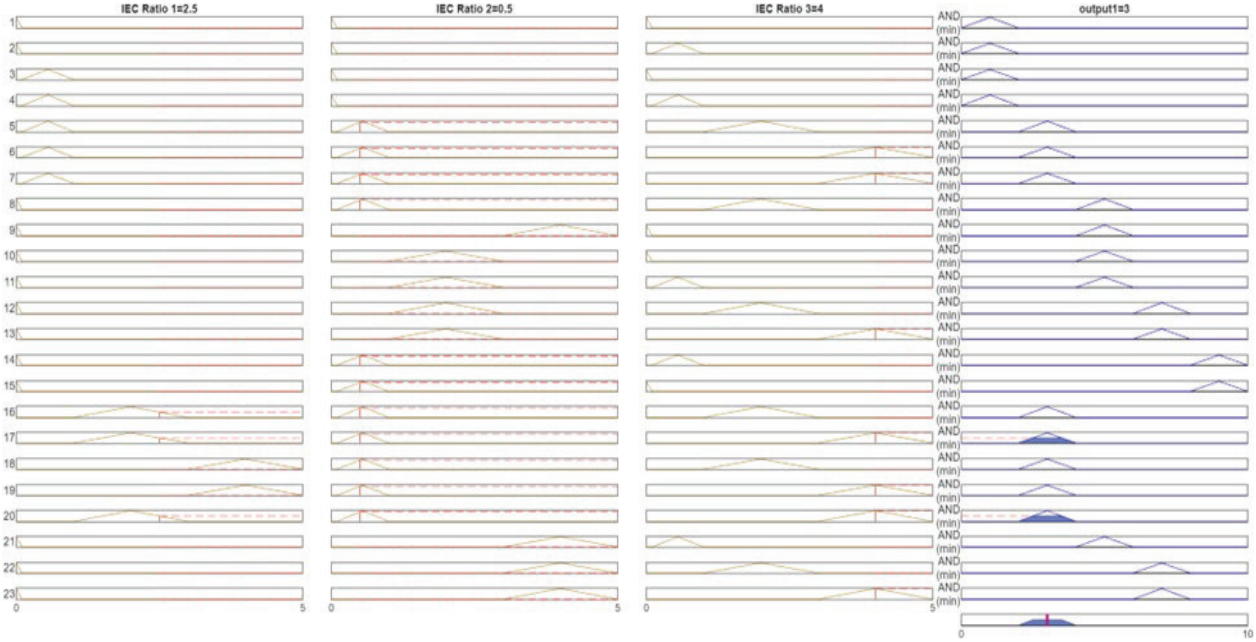

Fig. 3. Fuzzy Logic used in IEC ratio methods

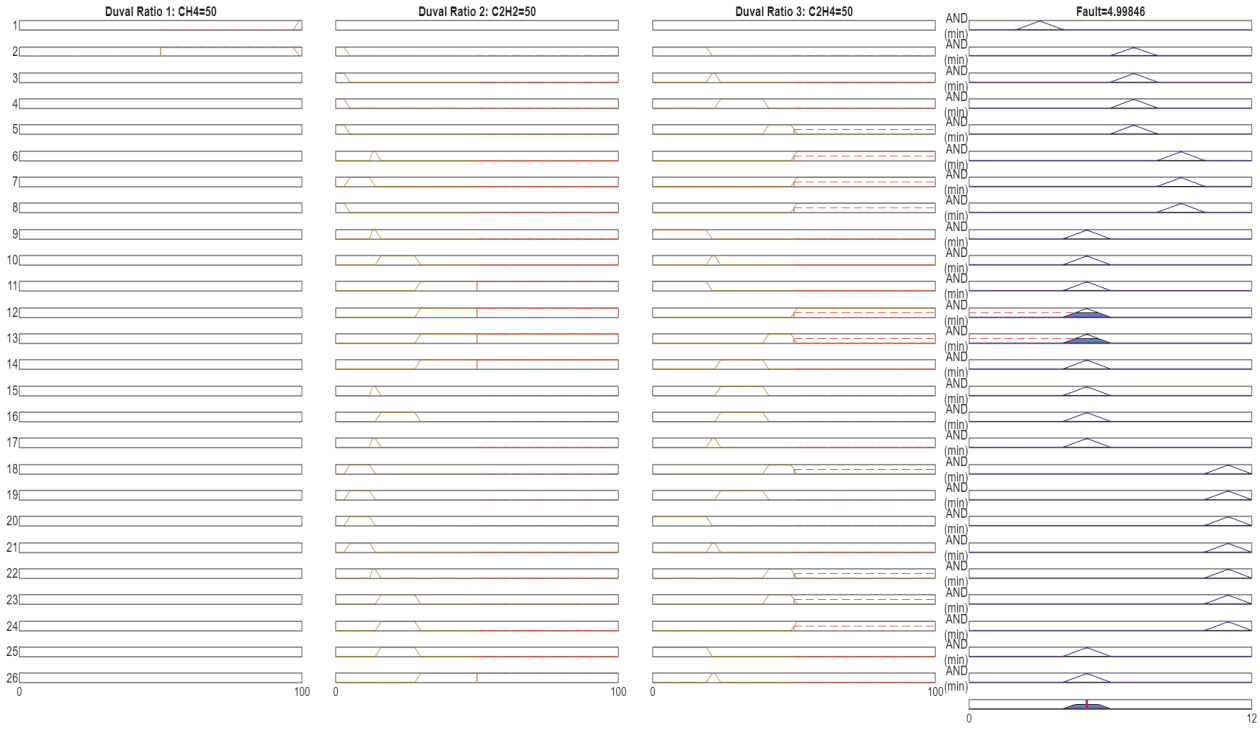

Fig. 4. Fuzzy Logic used in Duval Triangle

C. Performance evaluation of Fuzzy applied to DGA techniques

Table IV presents the results of both conventional Dissolved Gas Analysis (DGA) ratio integration methods and fuzzy logic based DGA techniques. A total of 27 samples were tested. The Duval method achieved an accuracy of 44%, while the Duval Fuzzy Inference System (FIS) yielded 26%, indicating no significant improvement when applying FIS to the Duval Triangle approach.

The least accurate method was the Doernenburg Fuzzy inference system, with an accuracy of only 11%. The IEC FIS outperformed its conventional counterpart. This improvement is attributed to the fuzzy model's ability to classify cases where the standard IEC method failed to produce an output.

Table IV: Performance comparison of the Fuzzy model approach and DGA ratio techniques (Adapted from [5], © IEEE [2026])

Sample No	H2	CH4	C2H6	C2H4	C2H3	IEC	IEC + FIS	Dornenburg	Dornenburg + FIS	Duval	Duval + FIS	Rogers	Rogers + FIS	Actual Fault	ANN
Sample 1	227	759	156	3133	191	NA	TL	TH	D	TH	TH	TH	TL	TH	TH
Sample 2	170	320	53	520	3	NA	TH	TH	D	TH	TH	TH	TL	TH	TH
Sample 3	650	53	34	20	0	PD	TL	PD	TL	TH	TH	PD	PD	PD	PD
Sample 4	300	490	180	360	95	NA	TL	TH	D	TH	TH	NA	TL	TH	D
Sample 5	117	167	48	481	7	NA	TL	TH	D	TH	TH	TH	TL	TL	TH
Sample 6	307	22	2	33	109	NA	TL	NA	TH	D	TH	NA	TL	D	PD
Sample 7	60	144	67	449	9	NA	TL	TH	D	TH	TH	TH	TH	TL	TL
Sample 8	208	1774	408	1431	1	NA	TL	TH	TL	TH	TH	TH	TL	TL	TL
Sample 9	75	15	7	14	26	D	TL	D	D	D	TH	NA	TL	D	D
Sample 10	1230	163	27	233	692	D	TL	D	TH	D	TH	D	TL	D	D
Sample 11	755	229	32	404	460	D	TL	D	D	D	TH	D	TL	D	D
Sample 12	105	125	71	166	10	NA	TL	TH	D	TH	TH	TH	N	N	PD
Sample 13	80	0	200	100	4	PD	TL	NA	TL	TH	TH	PD	PD	N	N
Sample 14	125	100	100	150	20	D	TL	NA	D	TH	TH	NA	TL	N	TH
Sample 15	50	30	0	0	5	D	TL	NA	D	D	D	NA	N	N	N
Sample 16	144	13	36	3	2	NA	TL	PD	TL	D	DT	NA	TL	PD	PD
Sample 17	503	40	25	14	0	PD	TL	PD	TL	TH	TL	PD	N	PD	PD
Sample 18	246	596	322	872	3	NA	TL	TH	D	TH	TH	TH	TH	TL	TL
Sample 19	1245	3865	721	2449	12	NA	TL	TH	D	TH	TH	TH	TH	TL	TL
Sample 20	35	78	29	210	5	NA	TL	TH	D	TH	TH	TH	TL	TL	N
Sample 21	546	1367	228	1196	14	NA	TL	TH	D	TH	TL	TH	TH	TH	TL
Sample 22	334	872	221	1481	37	NA	TL	TH	D	TH	TH	TH	TH	TH	TH
Sample 23	70	235	96	369	7	NA	TL	TH	D	TH	TH	TH	TL	TH	TH
Sample 24	730	1588	431	3972	74	NA	TL	TH	D	TH	TH	TH	TL	TH	TH
Sample 25	360	2933	23292	21341	94	TL	TL	TH	TL	TH	TH	NA	TL	TH	TH
Sample 26	52	31	3	1	5	TL	TL	NA	D	D	TL	NA	TL	N	N
Sample 27	107	91	79	157	36	D	D	NA	D	TH	TH	NA	TL	N	N
		Total Correct predictions				**5**	**7**	**14**	**3**	**12**	**7**	**10**	**8**		**20**
		Accuracy [%]				**19%**	**26%**	**52%**	**11%**	**44%**	**26%**	**37%**	**30%**		**74%**

Legend

Colour	Meaning
Green	Correct Predictions
Red	Incorrect predictions
Grey	no output

V. Application of the ANN on the Dataset

In this section the proposed ANN algorithm was evaluated on the data samples. Matlab™ R2000b simulation toolbox was used to simulate the supervised learning. Data pre-processing was conducted initially to pre-condition the dataset for the ANN classifier.

A. Data Pre-Processing

Prior to model development, the dataset underwent standard preparation procedures to improve data quality and model readiness. These included cleaning, transformation, scaling, and dimensionality reduction.

- **Rescaling**

A logarithmic transformation was applied to stabilise variations in gas concentrations and limit the effect of extreme values. The dataset contains a wide range of values, which can distort analysis if not appropriately transformed. The log transformation used in this study was calculated using equation (17):

$$Xlog = log10(1 + X) \tag{17}$$

Where *X* represents an individual gas concentration measured in ppm.
To avoid computational inconsistencies and errors, very small values were standardised to a minimum baseline.

- **Normalisation**

Input features were scaled within a fixed range to ensure balanced contribution during model training. This step ensures that variables with larger numerical ranges do not dominate those with smaller values. In this study, the scaling technique used is max – min normalization shown in (18).

$$Xnorm = \frac{X - Xmin}{Xmax - Xmin} \tag{18}$$

Xnorm represents the normalized value, *X* denotes the original value, *Xmin* is the minimum value of the feature, and *Xmax* is the maximum value of the feature.

- **Data Balancing**

Class imbalance was addressed by generating additional minority class samples to improve dataset representation. Although balancing techniques can enhance model performance, they may introduce bias and lead to overly optimistic accuracy, as the resulting model may not accurately represent real-world equipment conditions [14].

The ADASYN algorithm was implemented to increase the number of underrepresented fault cases. This method increased the dataset size from 145 to 273 samples, resulting in a more balanced distribution and improving the model's ability to recognize patterns.

- **Feature Selection**

Feature selection was applied to extract a smaller set of highly relevant variables from the original dataset. This process involved removing irrelevant, redundant, and noisy features to achieve a more simplified, efficient, and accurate model. Studies have indicated that integrating multiple feature selection techniques can lead to more robust and dependable outcomes [18]. In this work, PCA was used to determine appropriate features for the ANN classifier. Dimensionality reduction was performed to extract the most informative features from the dataset. Its advantages include reducing overfitting, lowering computational complexity, and enhancing model accuracy. In this study, PCA was implemented using a built-in MATLAB function as defined in equation (19):

$$[psc,scrs,\sim,\sim,pexp]=pca(Xlog) \tag{19}$$

Where *psc* returns p-by-k matrix, representing an initial value for coefficient, *scr,* a variance score returns a N-by -K matrix, representing the initial value for variance score,
pexp is percentage explained and *Xlog* is the input obtained from (17). The formula returns a vector containing percentage of the total variance explained by each principal component.

A reduced set of features capturing most of the dataset variance was retained for model input, improving efficiency without significant information loss as shown in Figure 5.

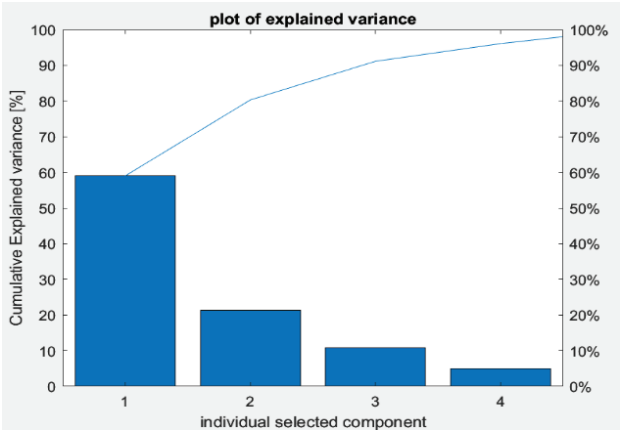

Fig. 5. PCA showing the variance in data (Adapted from [5], © IEEE [2026])

B. The ANN Architecture

The learning model was developed using a supervised training approach with regularisation applied to improve generalisation capability. The network configuration included a compact input layer, a single hidden layer, and an output layer designed to map fault categories.

- Evaluating the Neural Network with DGA Dataset

The sigmoid function was chosen as the activation function for this simulation and is mathematically defined in equation (20). It is within this function that the model performs its computations. The three inputs obtained from PCA are fed into the input layer and processed through the sigmoid function,

which evaluates them and carries out the necessary computations within the hidden layer.

$$F(x) = \frac{1}{1+e^{-x}} \tag{20}$$

where x represents the input value received at the input layer, while e is the mathematical constant equal to 2.718. The function $F(x)$ denotes the model's output. Table V presents the typical output in vector form as produced at the output layer, along with the corresponding fault classifications.

Table V: Fault code on the output layer

No	Fault code	Condition description
1	$[0\ 0\ 0\ 0\ 1]^T$	Normal degradation (N)
2	$[0\ 0\ 0\ 1\ 0]^T$	TL- Temperature fault <300
3	$[0\ 0\ 1\ 0\ 0]^T$	TH - Temperature fault>300
4	$[0\ 1\ 0\ 0\ 0]^T$	PD - Partial discharge of low and high energy
5	$[1\ 0\ 0\ 0\ 0]^T$	D – Arcing including discharge of low and high energy

- Training and Validation

Model development utilised separate subsets for training, validation, and testing to ensure reliable evaluation. The Bayesian Regularization algorithm was selected for training, with 1000 iterations and a target error of zero. Additionally, 20% of the dataset was used for validation to improve the classifier's ability to generalize.

- Testing the ANN Classifier

Once the classifier is trained using raw dataset, the testing dataset was then supplied to evaluate the classifiers' generalization performance. A total of 27 samples, representing 10% of the randomly selected dataset, were used to evaluate the ANN model's accuracy, with the results presented in Table VI. The limitations of the IEC, Doernenburg, and Rogers ratio methods are evident, as a total of 16, 6, and 9 samples, respectively, fall outside their classification ranges. Similarly, the Duval Triangle's tendency to detect faults even under normal operating conditions is demonstrated by 6 samples, which was incorrectly classified as faulty. Literature indicates that the Duval Triangle should only be applied when a fault is already evident, as it consistently predicts a fault condition, even for normal samples [1,19].
In contrast, the ANN classifier produced predictions for all test cases, with only a small number of misclassifications observed.

Figure 6 illustrates the results from Tables IV and VI, comparing the prediction accuracy of ANN, Doernenburg, Rogers, Duval, and IEC methods against the actual equipment conditions for each fault type. In general, the ANN based approach demonstrated more consistent predictive reliability compared to the traditional ratio based methods. It is also observed that integrating classical gas ratio techniques with a FIS does not significantly enhance their performance, except in the case of the IEC method, as shown in Figure 6. This observation supports the widely accepted view that no single diagnostic model is universally optimal for all scenarios [3].

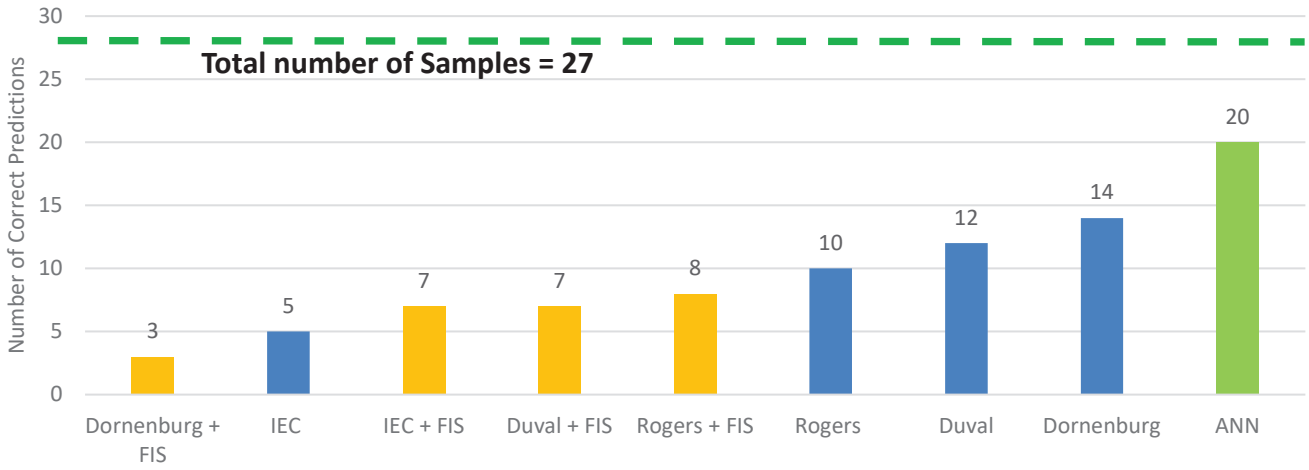

Fig. 6. Fault types per DGA method – performance comparison: correct predictions per technique, (Adapted from [5], © IEEE [2026])

Table VI: Comparison of ANN predicted results with actual condition (Adapted from [5], © IEEE [2026])

Sample No	H2	CH4	C2H6	C2H4	C2H3	IEC Faultcode	Dorn Faultcode	Duval Faultcode	Rogers Faultcode	Actual Fault	Predicted Fault
Sample 1	227	759	156	3133	191	NA	TH	TH	TH	TH	TH
Sample 2	170	320	53	520	3	NA	TH	TH	TH	TH	TH
Sample 3	650	53	34	20	0	PD	PD	TH	PD	PD	PD
Sample 4	300	490	180	360	95	NA	TH	TH	NA	TH	D
Sample 5	117	167	48	481	7	NA	TH	TH	TH	TL	TH
Sample 6	307	22	2	33	109	NA	NA	D	NA	D	PD
Sample 7	60	144	67	449	9	NA	TH	TH	TH	TL	TL
Sample 8	208	1774	408	1431	1	NA	TH	TH	TH	TL	TL
Sample 9	75	15	7	14	26	D	D	D	NA	D	D
Sample 10	1230	163	27	233	692	D	D	D	D	D	D
Sample 11	755	229	32	404	460	D	D	D	D	D	D
Sample 12	105	125	71	166	10	NA	TH	TH	TH	N	PD
Sample 13	80	0	200	100	4	PD	NA	TH	PD	N	N
Sample 14	125	100	100	150	20	D	NA	TH	NA	N	TH
Sample 15	50	30	0	0	5	D	NA	D	NA	N	N
Sample 16	144	13	36	3	2	NA	PD	D	NA	PD	PD
Sample 17	503	40	25	14	0	PD	PD	TH	PD	PD	PD
Sample 18	246	596	322	872	3	NA	TH	TH	TH	TL	TL
Sample 19	1245	3865	721	2449	12	NA	TH	TH	TH	TL	TL
Sample 20	35	78	29	210	5	NA	TH	TH	TH	TL	N
Sample 21	546	1367	228	1196	14	NA	TH	TH	TH	TH	TL
Sample 22	334	872	221	1481	37	NA	TH	TH	TH	TH	TH
Sample 23	70	235	96	369	7	NA	TH	TH	TH	TH	TH
Sample 24	730	1588	431	3972	74	NA	TH	TH	TH	TH	TH
Sample 25	360	2933	23292	21341	94	TL	TH	TH	NA	TH	TH
Sample 26	52	31	3	1	5	TL	NA	D	NA	N	N
Sample 27	107	91	79	157	36	D	NA	TH	NA	N	N

C. Further Evaluation of the ANN Model Performance Metrices

The model's performance was evaluated using metrics such as accuracy, specificity, precision, recall, and Mean Squared Error (MSE). It should be noted that on the Confusion Matrix, classes 1 to 5 correspond to the different output categories, defined as follows:

Class 1 – Partial Discharge (PD).

Class 2 – Discharge of low and high energy (D)

Class 3 – Thermal Temperature below 300°C (TH)

Class 4 – Thermal Temperature above 300°C (TH) and

Class 5 – Normal/ No Fault (N)



Fig. 7. Confusion Matrix for Training Data (Adapted from [5], © IEEE [2026])

- The Confusion Matrix

A confusion matrix was used to compare predicted and actual classifications. On its own, it is insufficient for fully evaluating model performance. Additional performance metrics, discussed in the subsequent sections, are required to obtain a comprehensive assessment.

Figures 7 and 8 illustrate the model's accuracy during the training and testing phases, respectively.

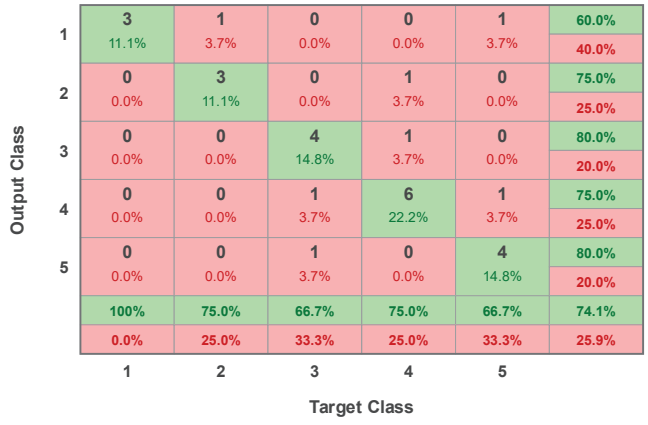

Fig. 8. Confusion Matrix for Testing Data (Adapted from [5], © IEEE [2026])

The horizontal axis represents the actual (target) output, while the vertical axis corresponds to the model's predicted output. Fault categories are indicated on the vertical axis using numerical labels from 1 to 5, where, for example, 1 represents Class 1 (Partial Discharge) as previously defined.

As illustrated in Figure 8, the testing results indicate correct prediction rates of 60% for Class 1 (Partial Discharge), 75% for Class 2 (Discharge), 80% for Class 3 (Low-temperature fault), 75% for Class 4 (High-temperature fault), and 80% for Class 5 (Normal condition). The model achieved an overall training accuracy of 92%, demonstrating strong pattern learning capability. However, when evaluated on new testing data, the accuracy decreased to 74%. Despite this reduction, the ANN model still outperforms conventional DGA methods.

- Mean Square Error (MSE)

The Mean Squared Error is determined by averaging the squared differences between the actual and predicted values, providing a measure of the model's prediction error. It indicates the extent of deviation between predicted and true values. During training, the model undergoes 1000 iterative epochs. As shown in Figure 9, the error for both training and testing datasets decreases as learning progresses. However, after approximately 190 epochs, overfitting begins to occur: the training error continues to decrease, while the testing error starts to increase. The classifier achieves its optimal performance at around 190 iterations, as depicted in the figure. Lower error values correspond to higher prediction accuracy.

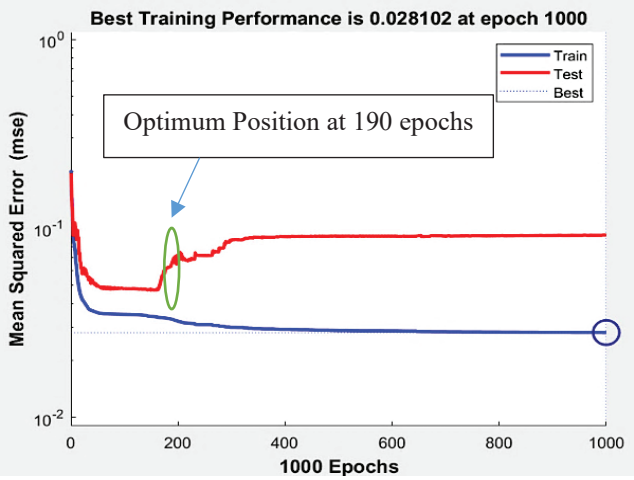

Fig. 9. Mean Square Error (Adapted from [5], © IEEE [2026])

- Receiver Operating Characteristic (ROC) Curve

The ROC curve in Figure 10 illustrates the true positive rate for the various fault classes. The diagonal line represents random classification, where the model correctly predicts the positive class only half of the time. The vertical axis indicates the model's true positive rate (correct classifications), while the horizontal axis shows the false positive rate (misclassifications). A curve closer to the vertical axis reflects better model accuracy and generalization. Although there is some variation in the model's positive prediction rates across classes, overall performance remains close to optimal, with results approaching a value of one.

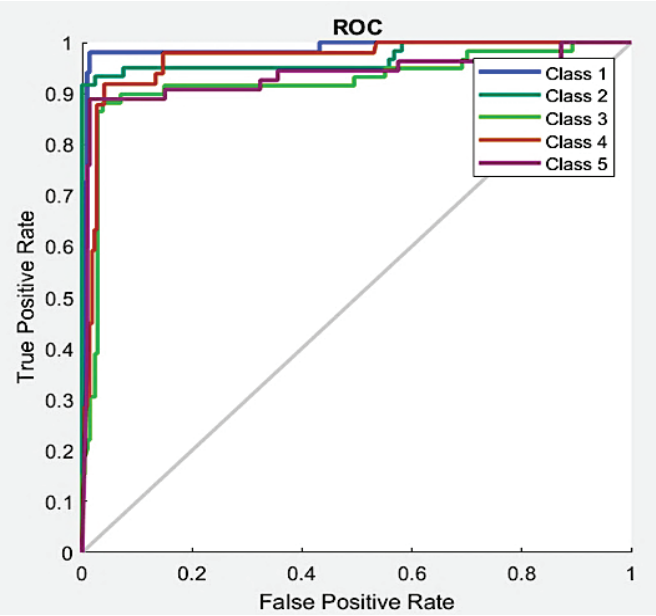

Fig. 10. Receiver Operating Characteristic Curve (Adapted from [5], © IEEE [2026])

- Accuracy

Accuracy simply refers to the percentage of correct predictions made by a classifier out of the total number of predictions. It is calculated using Equation (21), where *Tp, Tn, Fp and Fn* represents true positive, true negative, false positive and false negative, respectively.

.

$$Accuracy = \frac{Tp+Tn}{Tp+Tn+Fp+Fn} \text{ x } 100 \quad (21)$$

- Precision

Precision measures the proportion of true positive predictions relative to all predicted positive outcomes. It indicates how many of the positive predictions made by the model are actually correct and is defined by Equation (22).

$$\text{Precision} = \text{Tp}/(\text{Tp}+\text{Fp}) \text{ x } 100 \quad (22)$$

- Recall

Recall (also known as sensitivity or hit rate) measures the proportion of actual positive cases that are correctly identified by the model. It compares the true positives to all the positive instances in the ground truth and is expressed by Equation (23).

$$\text{Recall} = \text{Tp}/(\text{Tp}+\text{Fn}) \text{ x } 100 \quad (23)$$

- Specificity

Specificity (also referred to as selectivity) measures the proportion of actual negative cases that are correctly identified by the model. It reflects how effectively the model avoids false positive predictions and is expressed by Equation (24).

$$\text{Specificity} = Tn/(Tn+Fp) \times 100 \quad (24)$$

- Overall Performance

The overall performance of the ANN model is presented in Table VII. The model exhibits its highest predictive performance for PD and D faults, achieving average scores of 87% and 85%, respectively.

Table VII: Performance metrics of the ANN overall performance (Adapted from [5], © IEEE [2026])

fault type	Accuracy	Precision	Recall	Specificity	Average Performance
PD	89%	60%	100%	100%	87%
D	93%	75%	75%	96%	85%
TL	85%	80%	67%	91%	81%
TH	85%	75%	75%	89%	81%
N	89%	80%	67%	91%	82%

The thermal fault categories, low energy (TL) and high energy (TH), showed the lowest average performance at 81% each, indicating that the model had difficulty accurately identifying temperature related faults. As illustrated in the confusion matrix in Figure 8, the model accurately classified four TL fault cases (Class 3) but made two errors, misclassifying one as Normal (N) and another as a high-temperature fault (TH). This result is expected, as these categories lie close to each other along a continuous thermal spectrum. The case misclassified as Normal (N) likely represents a fault in its early stage, occurring at the boundary between normal condition and an evolving low-temperature fault. On the other hand, the case misclassified as TH may correspond to a more advanced fault nearing the transition between low and high temperature faults. In both cases, the model misclassified both borderline cases as low-temperature faults.

VI. Conclusion

The results of this study highlight the growing importance of intelligent algorithms in improving engineering diagnostic processes. In this work, the diagnostic data under consideration comprised DGA measurements from oil-filled power transformers. While a range of gas ratio analysis techniques have been developed and refined to the point of international standardization, this study shows that direct classification of gas ratios using a well-configured ANN algorithm can yield superior diagnostic efficacy compared to all conventional DGA classification methods evaluated.

The ANN based model achieved an average accuracy close to 77%, outperforming all conventional DGA techniques considered. Although integrating the IEC ratio method with a Fuzzy Inference System was found to improve upon the standalone IEC approach, this enhancement did not extend to the other conventional methods, further highlighting the relative advantage of the ANN-based approach.

Overall, these results suggest that machine learning techniques, and ANN models in particular, hold considerable promise for advancing the accuracy and reliability of transformer fault diagnosis, offering a compelling alternative to traditional rule-based classification frameworks.

VII. References

[1] S. Wani, A. Rana, S. Sohail, O. Rahman, S. Parveen, and S. Khan, "Advances in DGA based condition monitoring of transformers: A review," Renewable and Sustainable Energy Reviews, vol. 149, pp. 1–13, Oct. 2021.

[2] CIGRE Working Group D1/A2, "Advances in DGA Interpretation," CIGRE Technical Brochure 771, 2019.

[3] Mineral Oil-Filled Electrical Equipment in Service – Guidance on the Interpretation of Dissolved and Free Gases Analysis, IEC Standard 60599, IEC, Geneva, Switzerland, 2022.

[4] S. Ghoneim, I. Taha, and N. Elkalashy, "Integrated ANN-based proactive fault diagnostic scheme for power transformers using dissolved gas analysis," IEEE Transactions on Dielectrics and Electrical Insulation, vol. 23, no. 3, pp. 1838–1845, Jun. 2016.

[5] G. M. Mokgosi, C. Nyamupangedengu, and K. Nixon, "A comparative study on the accuracy of the conventional DGA techniques and artificial neural network classifiers of faults in oil filled power transformers," in Proceedings 33rd Southern African Universities Power Engineering Conference. (SAUPEC), Pretoria, South Africa, pp. 1–6, Jan. 2025.

[6] G. M. Mokgosi, "Comparative Study on the Accuracy of the Conventional DGA Techniques and Artificial Neural Network in Classifying Faults Inside Oil Filled Power Transformers," M.S. thesis, School of the Electrical and Information Engineering, University of the Witwatersrand, Johannesburg,South Africa, 2024.

[7] S. Wani, D. Gupta, M. Farooque, and S. Khan, "Multiple incipient fault classification approach for enhancing the accuracy of dissolved gas analysis (DGA)," IET Science, Measurement and Technology, vol. 13, no. 7, pp. 959–967, Jul. 2019.

[8] H. Yang and C. Liao, "Adaptive fuzzy diagnosis system for dissolved gas analysis of power transformers," IEEE Transactions on Power Delivery, vol. 14, no. 4, pp. 1342–1350, Oct. 1999.

[9] G. Rigatos and P. Siano, "Power transformers' condition monitoring using neural modeling and the local statistical approach to fault diagnosis," International Journal of Electrical Power and Energy Systems, vol. 80, no. 1, pp. 150–159, Sep. 2016.

[10] U. Rao, I. Fofana, K. Rajesh, and P. Picher, "Identification and application of machine learning algorithms for transformer dissolved gas analysis," IEEE Transactions on Dielectrics and Electrical Insulation, vol. 28, no. 5, pp. 1828–1835, Oct. 2021.

[11] Q. Su, C. Mi, L. Lai, and P. Austin, "A fuzzy dissolved gas analysis method for the diagnosis of multiple incipient faults in a transformer," IEEE Transactions on Power Systems, vol. 15, no. 2, pp. 593–598, May 2000.

[12] R. R. B. de Aquino, M. M. S. Lira, T. Filgueiras, H. Ferreira, O. N. Neto, A. M. S. Silva, and V. K. Asfora, "A fuzzy system for detection of incipient fault in power transformers based on gas-in-oil analysis," in Proceedings IEEE International Conference on Fuzzy Systems (FUZZ-IEEE), Barcelona, Spain, pp. 1–6, Jul. 2010.

[13] S. Islam, T. Wu, and G. Ledwich, "A novel fuzzy logic approach to transformer fault diagnosis," IEEE Transactions on Dielectrics and Electrical Insulation, vol. 7, no. 2, pp. 177–186, Apr. 2000.

[14] A. Abu-Siada, S. Hmood, and S. Islam, "A new fuzzy logic approach for consistent interpretation of dissolved gas-in-oil analysis," IEEE Transactions on Dielectrics and Electrical Insulation, vol. 20, no. 6, pp. 2343–2349, Dec. 2013.

[15] O. Gouda, S. El-Hoshy, and S. Ghoneim, "Enhancing the diagnostic accuracy of DGA techniques based on IEC-TC10 and related databases," IEEE Access, vol. 9, pp. 118049–118059, Aug. 2021.

[16] M. Duval, "Interpretation of gas-in-oil analysis using new IEC Publication 60599 and IEC TC 10 databases," IEEE Electrical Insulation Magazine, vol. 17, no. 2, pp. 31–41, Apr. 2001.

[17] H. Sun, Y. Huang, and C. Huang, "A review of dissolved gas analysis in power transformers," in Proceedings 2nd International Conference on Advances in Energy Engineering (ICAEE), Bangkok, Thailand, Dec. 2011, Energy Procedia, vol. 14, pp. 1220–1225, Dec. 2012.

[18] T. Kari, W. Gao, D. Zhao, K. Abiderexiti, W. Mo, Y. Wang, and L. Luan, "Hybrid feature selection approach for power transformer fault diagnosis based on support vector machine and genetic algorithm," IET Generation, Transmission and Distribution, vol. 12, no. 21, pp. 5672–5680, Nov. 2018.

[19] Standard Practices for Sampling Electrical Insulating Liquids, ASTM Standard D923, ASTM International, West Conshohocken, PA, USA, 2015.



Gomotsegang Mokgosi received her first degree in electrical engineering from the University of Cape Town in 2009. In 2024, she obtained an M.Sc. in Engineering at the University of the Witwatersrand South Africa. Gomotsegang has 16 years of experience in the Engineering industry, specializing in the asset management of high-voltage equipment. She currently holds the position of Senior Engineer at Exxaro Resource.



Cuthbert Nyamupangedengu (M'19) received his first degree in electrical engineering from the University of Zimbabwe in 1994. In 2004, he obtained an M.Sc. in Engineering at the University of the Witwatersrand South Africa, and in 2011 was awarded the Ph.D. Before moving to the University of the Witwatersrand, he was working with the Zimbabwe Electricity Supply Authority. Cuthbert is currently an associate professor and head of the School of the Electrical and Information Engineering, University of the Witwatersrand, South Africa, Johannesburg. He is an expert in partial discharge diagnosis. His research interests include high voltage engineering, insulation, power system planning and development, and nanotechnology.



Ken J. Nixon (M'06) Born in Johannesburg, South Africa in 1974. Received a BSc(Eng) degree in electrical engineering in 1996, an MSc degree in engineering in 1999 and a PhD degree in 2006, all from the University of the Witwatersrand, Johannesburg, South Africa. From 2001 to 2005, he was a Lecturer, and from 2006 to 2011, a Senior Lecturer, with the School of Electrical and Information Engineering. Since 2012, he has been an Associate Professor with the School of Electrical and Information Engineering, University of the Witwatersrand, Johannesburg, South Africa. His research interests include high voltage engineering, earthing and lightning protection, high performance computing, software engineering, applied machine learning and the sustainable use of energy.

CONTENTS PAGE